# A GENERAL AERODYNAMIC APPROACH TO THE PROBLEM OF DECAYING OR GROWING VIBRATIONS OF THIN, FLEXIBLE WINGS WITH SUPERSONIC LEADING & TRAILING EDGES AND NO SIDE EDGES

R. W. Warner — NACA, Ames Laboratory,
Moffett Field, California

---

## Abstract

The type of solution presented in this paper has extreme significance for the problem of flight flutter testing since the flutter characteristics of a flight vehicle could be checked analytically without actually penetrating the flutter region. For such a study indicial aerodynamic influence coefficients have several advantages. The indicial nature of the coefficients (responses to step function) makes them more readily applicable to decaying or growing motion than sinusoidal coefficients. In addition, aerodynamic influence coefficients can be applied to any plan form (within the limitations of the aerodynamic theory) and to any mode shape.

For the reasons stated above, indicial aerodynamic influence coefficients have been evaluated from potential theory for a thin, flexible wing with supersonic leading and trailing edges only. The analysis is based on the use of small surface areas in which the downwash is assumed uniform. Within this limitation, the results are exact except for the restriction of linearized theory. The areas are not restricted either to square boxes or Mach boxes. A given area may be any rectangle or square which may or may not be cut by the Mach forecone, and any area can be used anywhere in the forecone without loss of accuracy.

## INTRODUCTION

The purpose of this paper is to describe a feasible method for calculation of the aerodynamic forces due to arbitrary time-dependent downwash on flexible wings. Such aerodynamic forces have several important applications. They can provde the aero-dynamic forcing terms in gust problems. They can also give the aerodynamic terms due to decaying or growing vibrations that occur in the equations of motion for problems of gust response, airplane dynamic stability, and the approach to a flutter boundary. The latter application has significance for flight flutter testing since the flutter characteristics of a flight vehicle could be compared with analysis without actual penetration of the flutter region.

As with Pines and other authors (References 1 through 4), the present method is based on dividing the wing plan form into a number of discrete areas or boxes. In each of these areas the downwash is assumed to be uniform. In this paper a simplified approach is used to find the pressure at any point on the wing due to the downwash on each area in its Mach forecone. A variety of area shapes is permitted. By means of these so-called "aerodynamic influence co-efficients," arbitrary downwash distributions can be achieved for various plan forms. The present approach differs from the earlier methods primarily in its use of indicial aerodynamic influence coefficients. The adjective "indicial" means that the uniform downwash is applied suddenly to the area and maintained constant thereafter. The principal advantage of the indicial function is that it is a single function of time which can be superposed to give pressure for arbitrary time-dependent downwash. If sinusoidal functions were used to produce such downwash, both their real and imaginary parts would have to be superposed.

### The Indicial Aerodynamic Influence Coefficient for the Fundamental Area

In Figure 1, a general plan form with supersonic edges is outlined in dotted lines, with the flow passing over it at velocity V. A grid of small areas
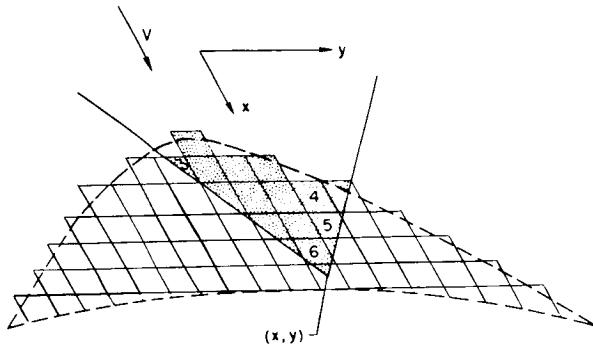
Figure 1. General Supersonic-Edged Plan Form with
Superimposed Grid

of uniform downwash is shown with solid lines and gives rise to a serrated leading edge in the approximation. The portions of those areas which can affect the pressure at a typical point (x, y) lie within the Mach forecone from that point and are shown shaded in Figure 1. Examples of these so-called "Mach forecone" areas are the polygons with three, four, five, and six sides, as numbered in Figure 1.

It has been found that aerodynamic influence coefficients for all the various polygons can be derived from the coefficient formula for a so-called "fundamental area" of uniform downwash. The fundamental area used herein consists of that portion of a representative quadrant in the plane of the wing (see Figure 2) which lies between the origin of the quadrant and one forward Mach line from (x, y). Thus the fundamental area is the shaded triangle in Figure 2. The point (x, y), where pressure is found, is taken to be in the plane of the wing and the triangle. The x', y' coordinates shown in Figure 2 are used only to locate the right-angle corner of the fundamental area
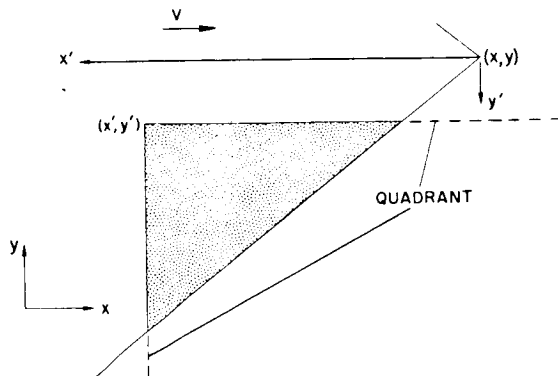
FUNDAMENTAL AREA



Figure 2. Fundamental Area

relative to the point (x, y), and these coordinates are prominent in the results which follow.

The exact indicial aerodynamic influence coefficients for such a fundamental area have been found by linearized theory. The result for $\frac{y'}{x'} \leq \frac{1}{M}$, where M is the free-stream Mach number, is presented in Figure 3 as the quantity $\left\{ \frac{\Delta P(t)}{W} \right\}$ in the right-hand column, with corresponding time zones indicated in the left-hand column. In Figure 3, $\Delta P(t)$ is the indicial pressure difference between the upper and lower surfaces of the wing at point (x, y), considered positive when it acts upward; W is the amount of uniform indicial downwash due to wing motion or gust velocity, positive downward; c is the speed of sound in the undisturbed medium; t is time; $\rho$ is the density of the undisturbed fluid; and $\beta$ is $\sqrt{M^2-1}$. One point to be noted in Figure 3 is the elementary nature of the functions. It should also be stated that if $\frac{y'}{x'} \geq \frac{1}{M}$, then the first two time zones are replaced by a single time zone for which $\left\{ \frac{\Delta P(t)}{W} \right\}$ is zero; and the other two zones are unaffected.

INDICIAL AERODYNAMIC INFLUENCE COEFFICIENT
FOR FUNDAMENTAL AREA IF y'/x'≦1/M



Figure 3. Indicial Aerodynamic Influence Coefficient
for Fundamental Area If y'/x' = 1/M

Application of the Indicial Aerodynamic Influence Coefficient for the Fundamental Area

The present calculations are based on application of the indicial aerodynamic influence coefficient for the fundamental area. The Mach box grid, such as that shown in Figure 4 for M = 1.6, is used. For this grid, introduced by Ta Li (References 2 and 3), the dimensions are $\lambda$ normal to the stream and $\beta\lambda$ parallel to the stream. The pressure is evaluated at the centroid of each box as, for example, at the apex of the Mach forecone shown in Figure 4. Hence, all Mach forecone areas of uniform downwash are triangles, like 10 and 47, or rectangles, like 14 and 39. As can be seen, the portion of the plan form
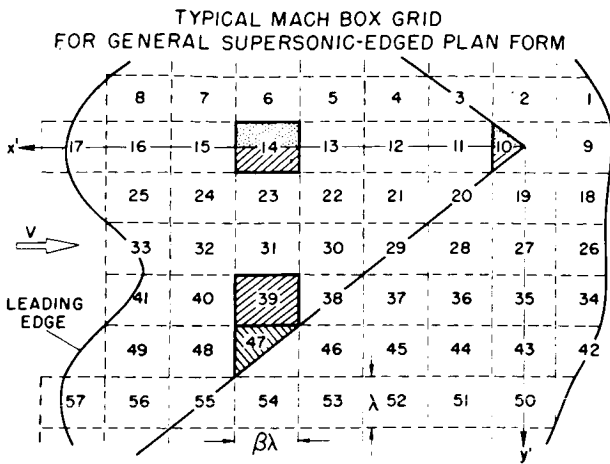
TYPICAL MACH BOX GRID
FOR GENERAL SUPERSONIC-EDGED PLAN FORM

Figure 4. Typical Mach Box Grid for General Super-
sonic-Edged Plan Form

shown in Figure 4 has a rather general shape. The
x' and y' axes, which define the right-angle corners
of fundamental areas, originate at the point where
pressure is sought.

Although the fundamental area shown in Figure
2 can be applied to more complicated Mach forecone
areas than are shown in Figure 4, its application to
areas such as 10, 47, 14, and 39 is representative.
The pressure difference at the Mach forecone apex
due to uniform indicial downwash on Mach forecone

area 10 is found by substituting $x' = \dfrac{\beta\lambda}{2}$ , $y' = 0$ into

the coefficient formula of Figure 3 to account for the
lower half of 10 in Figure 4 and doubling the result
to account for the upper half. For the triangular
(or fundamental) area 47, it is only necessary to sub-

stitute the values $x' = \dfrac{9\beta\lambda}{2}$ , $y' = \dfrac{7\lambda}{2}$ for the single

right-angle corner. For Mach forecone area 14 (see
Figures 4 and 5) one starts with the coefficient for
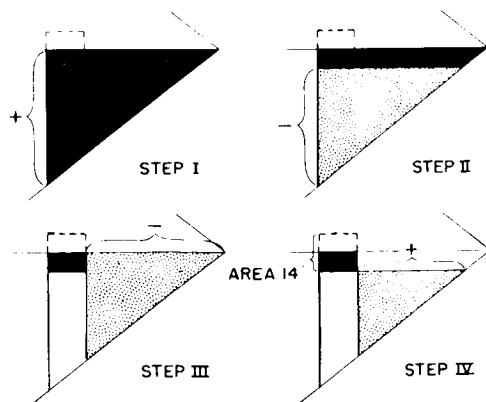
DEVELOPMENT OF THE COEFFICIENT FOR AREA 14

Figure 5. Development of the Coefficient for Area 14

the black triangle in step I of Figure 5. In a process
of superposition, one then subtracts the coefficients
for the shaded triangle in step II and the shaded tri-
angle in step III as indicated by the minus signs and
the braces in Figure 5. One then adds the shaded tri-
angle in step IV because this coefficient was sub-
tracted twice, once each in steps II and III. These
steps leave only the coefficient for the black rectangle
of step IV, which is the lower half of area 14; and this
result is doubled to account for the upper half. Since
all the fundamental areas used in these examples have

$\dfrac{y'}{x'} < \dfrac{1}{M}$, the coefficient formula of Figure 3 is used

without modification. It is essential, however, to
modify the coefficient in the manner previously de-

scribed when $\dfrac{y'}{x'} > \dfrac{1}{M}$.

The indicial influence coefficients for the four
Mach forecone areas shown shaded in Figure 4 are
plotted in Figure 6 against a dimensionless time,

$\dfrac{ct}{\lambda}$. The upper curve gives the pressure difference

at the apex of the Mach forecone in Figure 4 due to
uniform indicial downwash on Mach forecone area
10. This is the only curve having a non-zero initial
time zone since 10 is the only area containing the
point at which pressure is found. The other three
curves define the pressure differences at that point
due to Mach forecone areas 47, 14, and 39 as indicated
in Figure 6. The principal point to be noted is the
segmented nature of the curves.

If the transverse motion of the centroid of each
basic-grid box were considered to be a degree of
freedom in the equations of motion, results such as
those shown here would have to be used in the Duhamel
superposition integral for the analysis of decaying or
growing oscillations. The form of this integral, the
large number of degrees of freedom required, and
the irregular time histories of the indicial coefficients
would cause extreme difficulties in high-speed ma-
chine computation. If an analog machine were used,

TYPICAL INDICIAL AERODYNAMIC
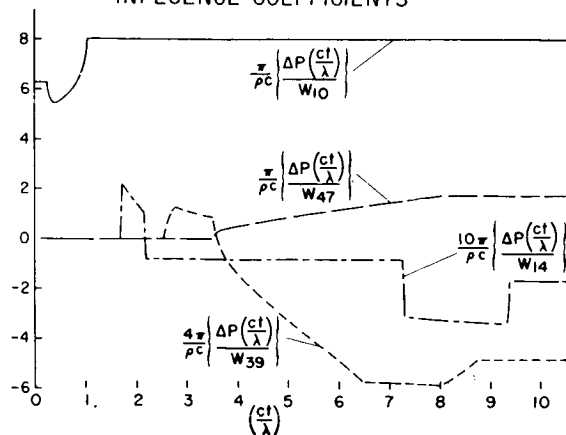INFLUENCE COEFFICIENTS

Figure 6. Typical Indicial Aerodynamic Influence
Coefficients

it would be essential to approximate these coefficients by a different set of exponentials for each of their segments. Although the exponential approximation would also facilitate digital computation, the use of a digital machine for such calculations would still require an extremely large memory. However, these indicial aerodynamic influence coefficients can be used relatively easily to evaluate generalized indicial forces. With these forces, relatively few degrees of freedom are required. In addition, a generalized indicial force is likely to be sufficiently smooth to be subject to approximation by one set of exponentials over its entire time history.

To determine the feasibility of applying indicial coefficients to the calculation of generalized indicial forces, a simple rigid-body example, for which exact theoretical results are known, will be presented. Consider a rigid, supersonic-edged delta wing at a Mach number of 1.2. The wing is shown in Figure 7 with dashed lines and has a leading-edge sweep of $24°$. The sweep has no bearing on the exact result for the delta wing but does influence the selection of boxes in the approximation. The wing is covered with 96 Mach boxes for M = 1.2, the box length normal to the stream being $\lambda$ and that parallel to the stream being $\dfrac{\beta\lambda}{2}$ for the trailing-edge boxes and $\beta\lambda$ for the rest, as indicated in Figure 7. The **uniform** pressure assumed over the trailing-edge boxes is evaluated at the trailing edge. For any pair of supersonic leading edges, the placing of the apex on the leading edge of the foremost box in the Mach box system has the principal advantage of minimizing the extent to which the boxes carry assumed constant pressure across the apex Mach lines, where the pressure distribution changes rapidly. Such an arrangement also alternates the carry-over of high pressure difference and low pressure difference, as with boxes 71 and 70, respectively, in Figure 7. The rule of thumb for discarding boxes along the leading edges is simply that boxes conforming to the pattern of the basic grid are included only if their centroids lie on the plan form of the delta wing.

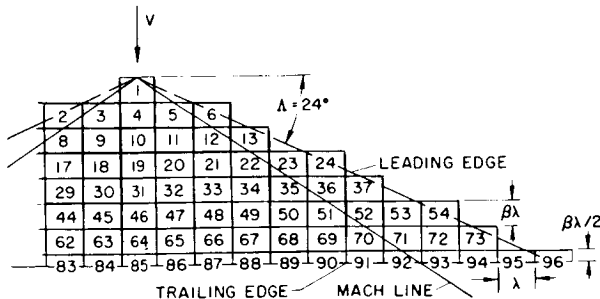SUPERSONIC-EDGED DELTA WING
WITH MACH BOX GRID FOR M = 1.2

Figure 7. Supersonic-Edged Delta Wing with Mach Box Grid for M = 1.2

It should be noted that the number of chordwise boxes at the maximum chord, namely eight, coincides with the minimum number recommended by Zartarian (Reference 5) for oscillatory functions. As he states, more boxes would be required if the chordwise deformation shape had more than one half-wave.

The generalized indicial force found for the delta wing just described is $C_{L_q}'$, that is, lift due to indicial pitching velocity, q, about the apex. In Figure 8 the lift is nondimensionalized in the usual fashion, and q is nondimensionalized with respect to the flow speed V, and the maximum chord $c_0$. In the present approximation, the uniform downwash on each box due to q is evaluated at the centroid of each box except for the trailing-edge boxes, where the trailing edge is the reference for downwash as well as pressure. The time is made dimensionless in this case by the flow speed V and the maximum chord $c_0$.

LIFT DUE TO INDICIAL PITCHING OF A
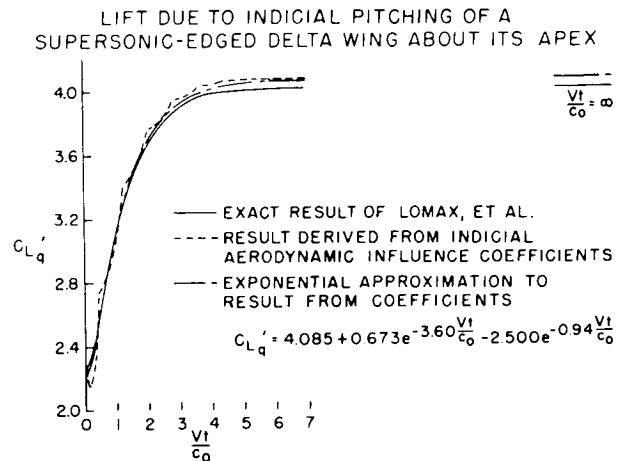SUPERSONIC-EDGED DELTA WING ABOUT ITS APEX

Figure 8. Lift Due to Indicial Pitching of a Supersonic-Edged Delta Wing About Its Apex

Figure 8 contains three curves: the exact theoretical result taken from Reference 6, the curve derived from the indicial aerodynamic influence coefficients, and an exponential approximation based on points taken from the curve determined by the influence coefficients. The irregularities in the curve derived from the coefficients are the result of using a finite number of boxes. The exponential approximation is in error relative to the exact result by a maximum of nearly 2 percent.

The question arises as to whether such a good exponential curve fitting could have been accomplished if the exact result had not been known in advance. Fortunately, a large part of the curve-fitting procedure is quite general and does not require specific knowledge of the exact result. The first step is to select from the function determined by the indicial coefficients a set of points upon which the exponential approximation is to be based. In the present case, the points chosen were those whose abscissas lie halfway between the peaks of the ser-

rated curve in Figure 8, with the valley nearest time zero excluded. (The initial time zone will be discussed later.) In addition, the initial $\left(\dfrac{Vt}{c_0} = 0\right)$ and steady-state $\left(\dfrac{Vt}{c_0} = 6\right)$ points of the serrated curve were used. The valley points were chosen, rather than peak or mean values, because one would expect the exact function to be smaller than the function based on the coefficients even if the exact function were not known. This results from the fact that the total area of the boxes is approximately 1 percent greater than the actual delta-wing area. Furthermore, the evaluation of the downwash right at the trailing edge gives somewhat too high a uniform downwash over the half boxes on the trailing edge. Such a procedure for the selection of points upon which to base the exponential approximation in all but the earliest time region would be expected to apply to more complicated plan forms and mode shapes.

The second step in the exponential curve fitting is the application of judgment as to the nature of the indicial function in the earliest time region. This step is aided by the general knowledge that all the various supersonic indicial functions calculated for specific plan forms and mode shapes in References 6 and 7 have one or more inflection points near time zero. However, some of the functions have one point of inflection without a dip, and some have two points of inflection with a dip. Thus the rejection of the first valley in the serrated curve of Figure 8 and the subsequent selection of the exponential approximation with only an indistinguishable dip, essentially at time zero, required knowledge of the exact result for the present case. For more general indicial functions, then, the decision as to whether to ignore the dip may give rise to an error as large as 10 percent in the earliest time region. This potential error can be reduced, of course, by developing usable points closer to time zero. The principal means of doing this is the use of a larger number of boxes, which would improve accuracy over the entire time span.

Once the points to approximate have been selected and the behavior near time zero has been estimated, the third step is the actual exponential approximation. Two exponentials and a constant term are used for the example in Figure 8. The constant term is the steady-state value derived from the indicial coefficients. It can be adjusted according to the relative areas of the boxes and the actual wing if desired. One of the exponentials is adjusted to fit the points to be approximated at the higher values of time. The other exponential, having a larger exponent, is used to match the desired properties near time zero and damp out at larger times. Such a procedure will probably suffice for more general indicial functions than that of Figure 8.

As a check on the adequacy of the particular exponential approximation in Figure 8, a frequency response is computed over the limited range of re-

duced frequency, $\dfrac{\omega c_0}{2V}$, for which the necessary tabulated functions are generally available. The exact results for $C_{L_{q(\text{real})}}'$ and $C_{L_{q(\text{imag})}}'$, based on an integral evaluated in reference 8 in terms of functions tabulated in Reference 9, are plotted against $\dfrac{\omega c_0}{2V}$ in Figure 9. The results of introducing the exponential approximation of Figure 8 in the Duhamel integral and specializing for sinusoidal motion are also shown in Figure 9. The maximum percentage discrepancy between the approximate and the exact results occurs at the very small values of $C_{L_{q(\text{imag})}}'$ near $\dfrac{\omega c_0}{2V} = 2.0$. Elsewhere, the largest errors are around 3 percent, which is considered quite good.

COMPARISON OF EXACT AND APPROXIMATE
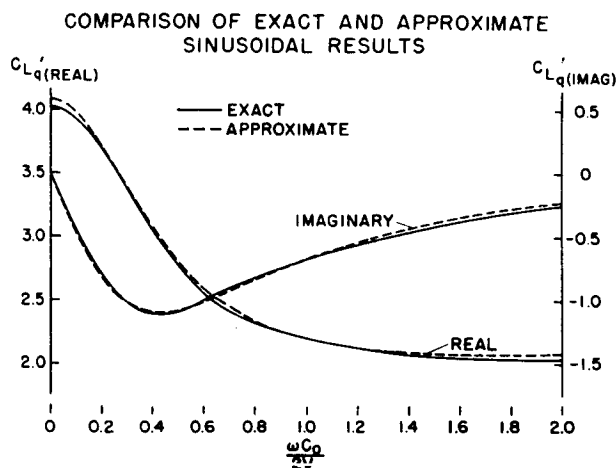SINUSOIDAL RESULTS



Figure 9. Comparison of Exact and Approximate Sinusoidal Results

CONCLUSION

In view of the foregoing results and discussion, it appears that the application of generalized indicial forces, derived from indicial aerodynamic influence coefficients, to the problem of predicting decay rates in flight flutter testing will be feasible.

REFERENCES

1. Pines, Samuel, Dugundji, John, and Neuringer, Joseph: Aerodynamic Flutter Derivatives for a Flexible Wing with Supersonic and Subsonic Edges. Jour. Aero. Sci., vol. 22, no. 10, Oct. 1955, pp. 693-700. (See also Pines, S., and Dugundji, J.: Aerodynamic Flutter Derivatives of a Flexible Wing with Supersonic Edges. Aircraft Ind. Assoc. ATC Rep. No. ARTC-7, Feb. 15, 1954. Pines, S., and Dugundji, J.: Application of Aerodynamic Flutter Derivatives to Flexible Wings with Supersonic and Subsonic Edges. Republic Aviation Corp. Rep. E-SAF-2, Apr. 1954)

2. Li, Ta C. H.: Aerodynamic Influence Coefficients for an Oscillating Finite Thin Wing. Chance Vought Aircraft, Inc., CVA Rep. No. 9513, Aug. 23, 1954.

3. Li, TA: Aerodynamic Influence Coefficients for an Oscillating Finite Thin Wing in Supersonic Flow. Jour. Aero. Sci., vol. 23, no. 7, July 1956, pp. 613-622.

4. Voss, H. M., Zartarian, G., and Hsu, P. T.: Application of Numerical Integration Techniques to the Low-Aspect-Ratio Flutter Problem in Subsonic and Supersonic Flows. M.I.T. Aeroelastic and Structures Research Laboratory Technical Report 52-3, Contract NOa(s) 53-564-c for Bureau of Aeronautics, USN, Oct. 1954.

5. Zartarian, Garabed: Theoretical Studies on the Prediction of Unsteady Supersonic Airloads on Elastic Wings. Part 2. Rules for Application of Oscillatory Supersonic Aerodynamic Influence Coefficients. WADC Tech. Rep. 56-97, Part II, ASTIA Doc. No. AD 110592, Feb. 1956.

6. Lomax, Harvard, Heaslet, Max. A., Fuller, Franklyn B., and Sluder, Loma: Two- and Three-Dimensional Unsteady Lift Problems in High-Speed Flight. NACA Rep. 1077, 1952. (Supersedes NACA TN's 2256, 2387, and 2403)

7. Lomax, Harvard, Fuller, Franklyn, B., and Sluder, Loma: Generalized Indicial Forces on Deforming Rectangular Wings in Supersonic Flight. NACA Rep. 1230, 1955. (Supersedes NACA TN 3286)

8. Tobak, Murray: On the Minimization of Airplane Responses to Random Gusts. NACA TN 3290, 1957.

9. Huckel, Vera: Tabulation of the $f_\lambda$ Functions Which Occur in the Aerodynamic Theory of Oscillating Wings in Supersonic Flow. NACA TN 3606, 1956.